



25th ABCM International Congress of Mechanical Engineering
October 20-25, 2019, Uberlândia, MG, Brazil

COB-2019-1882

A COMPARISON BETWEEN MODELING STRATEGIES FOR THE TORSIONAL DYNAMICS OF DRILL-STRINGS USING LUMPED-PARAMETER MODELS

Daniel de Moraes Lobo

Thiago Gamboa Ritto

Felipe Dias Massa

Universidade Federal do Rio de Janeiro, Department of Mechanical Engineering, Rio de Janeiro, Brazil
daniel.lobo23@poli.ufrj.br, tritto@mecanica.ufrj.br, felipediasmassa97@poli.ufrj.br

Abstract. *Drill-strings are slender tubular structures used in drilling operations. This structure is often subjected to severe vibrations that can cause even the complete failure of the structure. One of the most harmful vibrations is the torsional one. Many authors have proposed lumped parameter models to describe the torsional dynamics of drill-strings, but there is still a lack of investigations about the comparison between the modeling strategies proposed. These investigations usually focus on the bit-rock interaction but neglect the discretization and other subjects. The objective of this work is to investigate different discretization strategies and compare them in terms of the natural frequencies. Also, the advantages of using dimensionless equations are discussed. It is concluded that a better discretization of the drill-pipes is more helpful and the use of dimensionless quantities generate results less sensitive to changes in drill-string properties.*

Keywords: *drill-string, lumped parameter model, stick-slip, torsional dynamics*

1. INTRODUCTION

Drill-strings are slender tubular structures used to drill holes in the earth's surface in order to reach petroleum reservoirs. It is composed of two main sections: the drill-pipes (DPs), which are slender tubes that can reach several kilometers, and; the bottom-hole-assembly (BHA), which have several hundred meters and is composed of thicker tubes and other equipment. This structure is subjected to severe vibrations during the drilling operation and these vibrations are classified into axial, torsional and lateral vibration. The torsional vibration is one of the most harmful ones and can cause different problems during operation, even the complete failure of the drill-string. The severest torsional vibration is commonly referred as 'stick-slip' and it describes the situation in which the bit presents a very large variation in rotational speed while the top of drill-string rotates at an almost constant rotational speed.

Several models have been proposed in the literature to describe the torsional dynamics of drill-strings (Saldivar *et al.*, 2016). Some of these models consider only the torsional dynamics (Ritto *et al.*, 2017; Navarro-lópez *et al.*, 2004), while others consider also the coupling with axial and lateral dynamics (Hong *et al.*, 2016; Richard *et al.*, 2007). Despite its simplicity uncoupled torsional models can describe pretty well the torsional dynamics of drill-strings when the other vibrations are small (Ritto *et al.*, 2017). Regarding torsional dynamics, two kinds of model are found in literature: continuum models and lumped-parameter models. Although lumped-parameter models are very simple, they are very useful and can describe a lot of important phenomena that happen during drilling. In addition, some models consider only one degree of freedom (DOF) (Richard *et al.*, 2007) for torsional dynamics, while others consider more DOFs to describe the BHA (Ritto *et al.*, 2017; Hong *et al.*, 2016; Navarro-López and Cortés, 2007). Although there are many models available in the literature, there is still a lack of discussion about what is the best strategy to discretize the drill-string in order to use lumped-parameter models.

Besides, although many authors consider dimensional quantities in the model (Lobo *et al.*, 2017; Kamel and Yigit, 2014; Tang *et al.*, 2015), the use of dimensionless quantities can elucidate important relations of the problem (Nandakumar and Wiercigroch, 2013; Yigit and Christoforou, 1998; Germy *et al.*, 2009). Despite this, the advantage of using dimensionless quantities in pure torsional models has never been assessed.

Motivated by the above findings, the objectives of this work are: (i) to study the different strategies used to model the torsional dynamics of drill-strings using lumped-parameter models, and; (ii) to propose a dimensionless equation of motion in order to assess the advantage of using dimensionless quantities.

This article is organized as follows. In section 2, the mathematical model is presented and the discretization strategies are explained. In addition, the dimensionless quantities are defined and the dimensionless equation of motion is presented.

In section 3, the natural frequencies obtained using lumped parameter models are compared with the ones obtained with the finite element method. Also, the advantage of using dimensionless quantities is discussed through the map of torsional vibration severity, which is evaluated for the model using dimensional and dimensionless quantities.

2. MATHEMATICAL MODEL

The mathematical model used in this work is illustrated in Fig. 1, which compares the continuum case with the discrete case. A constant rotational speed Ω is applied at the top of drill-string ($i = 0$) and the bit-rock interaction is included by a torque T_{bit} on the last inertia ($i = N$).

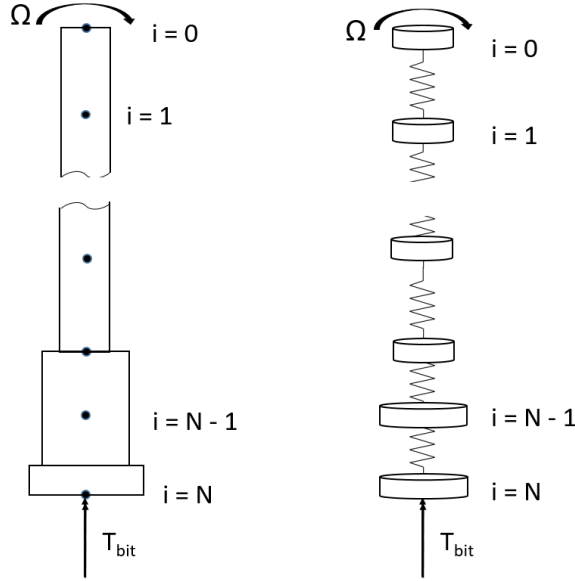


Figure 1: Schematic view of torsional lumped-parameter model.

In the case with 1 degree-of-freedom (dof), i.e. $i = 1$, the equation of motion is written as:

$$I\ddot{\theta}_{bit}(t) + c\dot{\theta}_{bit}(t) + k\theta_{bit}(t) = -T_{bit}(\dot{\theta}_{bit}(t)) + c\Omega + k\Omega t, \quad (1)$$

where $\theta_{bit}(t)$ is the rotational angle of the bit; I is the moment of inertia, and; k and c are the stiffness and damping that connect the lumped elements $i = 0$ and $i = 1$. Note that the motion is prescribed in $i = 0$ and, thus, it does not represent a dof. $T_{bit}(\dot{\theta}_{bit}(t))$ is the torque due to bit-rock interaction, which is modeled according to Tucker and Wang (1997):

$$T_{bit}(\dot{\theta}_{bit}(t)) = W_{ob}R_{bit}a_0 \left(\tanh(a_1\dot{\theta}_{bit}(t)) + \frac{a_2\dot{\theta}_{bit}(t)}{1 + a_3\dot{\theta}_{bit}^2(t)} \right), \quad (2)$$

where W_{ob} is the weight-on-bit; R_{bit} is the equivalent radius of the bit, and; a_0 to a_3 are constants obtained from calibration. In the case with multiple degrees-of-freedom, the dimension of the equation of motion increases and it becomes:

$$[I]\{\ddot{\theta}(t)\} + [C]\{\dot{\theta}(t)\} + [K]\{\theta(t)\} = \begin{bmatrix} c_1\Omega + k_1\Omega t \\ 0 \\ \vdots \\ 0 \\ -T_{bit}(\dot{\theta}_{bit}(t)) \end{bmatrix} \quad (3)$$

where $[I]$ is the inertia matrix; $[K]$ is the stiffness matrix; $[C]$ is the damping matrix, which is assumed to be proportional to inertia and stiffness matrices, i.e. $[C] = \alpha[I] + \beta[K]$; c_1 and k_1 are the damping and stiffness in the connection between lumped elements $i = 0$ and $i = 1$. Note that the terms with k_1 and c_1 arises from the boundary condition of constant speed at the $i = 0$.

2.1 Stiffness calculation

The torsional stiffness k_i connecting each pair of lumped elements is defined as:

$$k_j = \frac{G J_j}{L_j}, \quad 1 < j < N, \quad (4)$$

where G is the shearing modulus, J_j is the polar moment of inertia and L_j is the length of the section j between elements $i = j$ and $i = j - 1$.

2.2 Inertia calculation

Although the calculation of stiffness is pretty straightforward, there are three main strategies used to calculate the moment of inertia I_i of the degree of freedom i . The first strategy (called A in this work) is a very common strategy used for 1-DOF models. This strategy assumes the BHA as a rigid body and the moment of inertia is expressed as:

$$I = \frac{1}{3}I_{DP} + I_{BHA}, \quad (5)$$

where I_{DP} is the moment of inertia of the drill-pipes and I_{BHA} is the moment of inertia of the BHA. This strategy has been extensively used in the literature Lobo *et al.* (2017); Navarro-lópez *et al.* (2004); Richard *et al.* (2007) when the torsional dynamics is represented by a single lumped element. The proof of this approximation is available in J. P. Den Hartog (1947).

The second strategy (B) consists on assigning half of the moment of inertia of section j to the lumped elements on the extremities of this section ($i = j$ and $i = j - 1$). The moment of inertia (I_j^*) of each section j is written as $I_j^* = \rho J_j L_j$ and the inertia matrix can be written for N DOFs as:

$$[I] = \begin{bmatrix} I_1^*/2 + I_2^*/2 & 0 & \cdots & 0 & 0 \\ 0 & I_2^*/2 + I_3^*/2 & \cdots & 0 & 0 \\ \vdots & \vdots & \ddots & \vdots & \vdots \\ 0 & 0 & \cdots & I_{N-1}^*/2 + I_N^*/2 & 0 \\ 0 & 0 & \cdots & 0 & I_N^*/2 \end{bmatrix}. \quad (6)$$

The third strategy (C) is very similar to strategy B, but it considers the BHA as a rigid body. This is motivated by the hypothesis made in strategy A, which is adopted in many works. Considering the BHA as rigid, the BHA inertia is added to the last term of inertia matrix:

$$[I] = \begin{bmatrix} I_1^*/2 + I_2^*/2 & 0 & \cdots & 0 & 0 \\ 0 & I_2^*/2 + I_3^*/2 & \cdots & 0 & 0 \\ \vdots & \vdots & \ddots & \vdots & \vdots \\ 0 & 0 & \cdots & I_{N-1}^*/2 + I_N^*/2 & 0 \\ 0 & 0 & \cdots & 0 & I_N^*/2 + I_{BHA} \end{bmatrix}. \quad (7)$$

In the case of 1-dof model, this strategy would give the following inertia:

$$I = \frac{1}{2}I_{DP} + I_{BHA}. \quad (8)$$

2.3 Dimensionless formulation

The next step is to transform Eq. 3 into a dimensionless equation. To do this, we define the following equivalent stiffness:

$$k_{eq} = \frac{1}{[K]_{N,N}^{-1}}, \quad (9)$$

where $[K]_{N,N}^{-1}$ is the last term in the diagonal of the inverse of the stiffness matrix. The equivalent stiffness k_{eq} is the stiffness of a 1-DOF model that would give the same total torsion as the N-DOF model if a constant torque is applied at the last element. In addition, we define the equivalent inertia

$$I_{eq} = \frac{k_{eq}}{\omega_1^2}, \quad (10)$$

where ω_1 is the first torsional natural frequency. Introducing the dimensionless time $\tau = \omega_1 t$ in Eq. 3 and dividing by the equivalent stiffness k_{eq} , we obtain the dimensionless equation:

$$[\mathbb{I}]\{\ddot{\theta}(\tau)\} + [\mathbb{C}]\{\dot{\theta}(\tau)\} + [\mathbb{K}]\{\theta(\tau)\} = \begin{bmatrix} \mathbb{C}_1 \Pi_1 + \mathbb{K}_1 \Pi_1 \tau \\ 0 \\ \vdots \\ 0 \\ -b_0 \Pi_2 \left(\tanh(b_1 \dot{\theta}(\tau)) + \frac{b_2 \dot{\theta}(\tau)}{1 + b_3 \dot{\theta}^2(\tau)} \right) \end{bmatrix} \quad (11)$$

where $[\mathbb{I}] = \frac{[I]}{I_{eq}}$ is the dimensionless inertia matrix; $[\mathbb{C}] = \frac{[C]\omega_1}{k_{eq}}$ is the dimensionless damping matrix; $[\mathbb{K}] = \frac{[K]}{k_{eq}}$ is the dimensionless stiffness matrix; $\mathbb{C}_1 = \frac{c_1 \omega_1}{k_{eq}}$ and $\mathbb{K}_1 = \frac{k_1}{k_{eq}}$ are the dimensionless damping and stiffness of the first section; $\Pi_1 = \frac{\Omega}{\omega_1}$ and $\Pi_2 = \frac{W_{ob} R_{bit}}{k}$ are dimensionless quantities; $b_0 = a_0$, $b_1 = \omega_1 a_1$, $b_2 = a_2$ and $b_3 = \omega_1^2 a_3$ are the dimensionless constants of bit-rock interaction model.

3. RESULTS

The results presented in this section consider the drill-string data depicted in Tab. 1 and the following properties: $G = 85.3 \times 10^9$ Pa; $\rho = 7800$ kg/m³; $a_0 = 0.221$; $a_1 = 0.2$ s; $a_2 = 0.89$ s; $a_3 = 0.06$ s². The drill-bit is considered rigid in all the cases studied. The equations of motion are solve using "ode45" in MATLAB.

Table 1: Drill-string data used in simulations. Adopted from (Ritto *et al.*, 2017).

Section	Description	D_{out} [m]	D_{ins} [m]	L [m]
DP	Drill pipes 5 1/2"	0,140	0,119	4733,6
BHA 1	HWDP 5 1/2"	0,140	0,076	171,30
BHA 2	Drill collars, MWD tools & LWD tools 6 3/4"	0,171	0,071	294,90
BIT	Drill-bit 8 1/2"	0,216	0,057	0,25

The strategies A, B and C were used to discretize the drill-string into a lumped parameter model. The natural frequencies are obtained by solving the following generalized eigenvalue problem and compared with the ones obtained by using the finite element method (FEM) in ABAQUS with 2430 elements. Using strategy A, i.e. with 1 DOF and rigid BHA, the first natural frequency obtained (1.1344 Hz) returned a difference of 2.8 % in respect to the FEM result (0.1307 Hz). A comparison between the mode shapes calculated with this strategy and with the FEM is presented in Fig.2. The mode shapes are very similar, especially in the BHA. Although this strategy cannot capture all the details of the mode shape in the DPs, the difference to the FEM result is small. Thus, this strategy presents a good simplification of the problem.

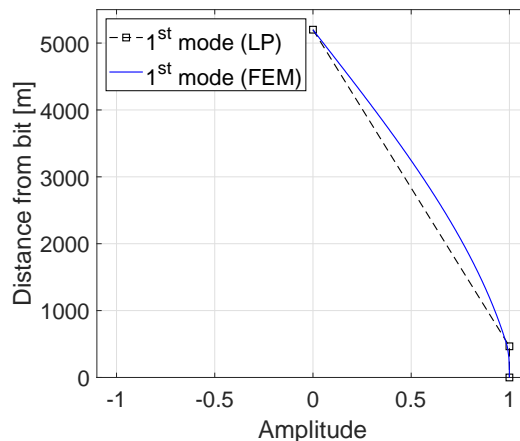


Figure 2: Mode shape of the first mode when the strategy A is used (BHA is rigid and DP has 1 DOF).

Using strategy C, one can discretize the DPs in multiples DOFs, maintaining the BHA as a rigid body. Figure 3(a) shows a comparison between the natural frequencies obtained with strategy C with the ones obtained with FEM for the first three vibration modes. It is shown that the first natural frequency is predicted very well with few DOFs and the 2nd and 3rd natural frequencies converge to the ones calculated with FEM. Thus, strategy C works pretty well for the lowest vibration modes. The mode shapes of the first and second modes are shown in Fig. 3(b) for the case in which the DPs are discretized in 5 DOFs. The compatibility between the mode shapes calculated by using strategy C and FEM is verified.

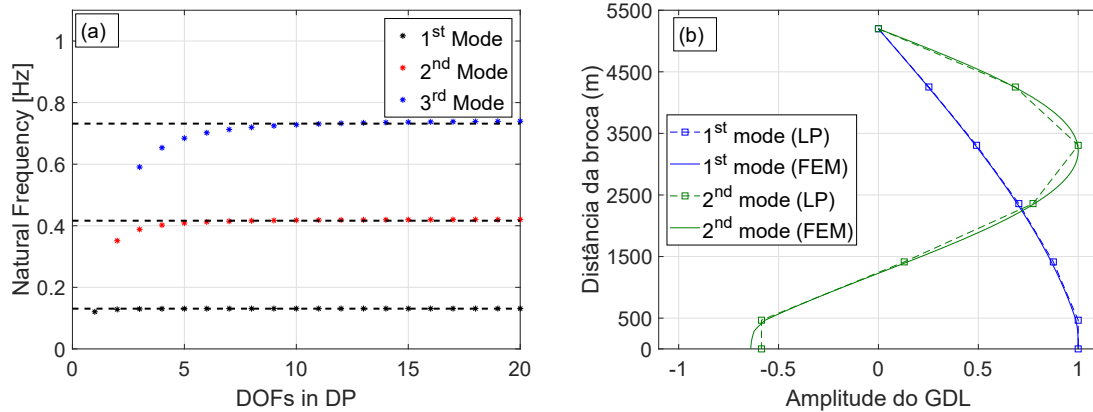


Figure 3: (a) Comparison between natural frequencies obtained with the lumped parameter model (LP) and the ones obtained by FEM (horizontal dashed lines). The BHA is rigid and only the DPs are discretized. (b) Mode shapes calculated for the first and second modes with the DPs discretized in 5 DOFs and BHA rigid.

A common approach used in literature is to discretize the BHA in multiple DOFs and keep the DPs with one DOF. It is maybe motivated by the fact that the BHA is composed of many different sections. This approach is equivalent to use strategy B with only 1 DOF in the drill-pipes (DP). Figure 4(a,b) shows the comparison between the natural frequencies obtained using this strategy with the ones obtained with FEM. It is noticed that the second natural frequency converges to a frequency which does not exist in FEM results. The third natural frequency converges to a value closer to the result obtained with FEM. Note that the second and third modes here comes from the second and third eigenvalues calculated with strategy C and they do not correspond to the second and third frequencies obtained with FEM. The first natural frequency is not shown because the discretization of BHA does not affect the first natural frequency, which remains with a difference of 8% with respect to the FEM results. The mode shapes are shown in Figure 4(c) and it is noticed that the shape is pretty well captured in the BHA, but there are high amplitudes in the DPs which are neglected. Thus, it is concluded that the discretization of the BHA is not worth it when the DPs are not discretized as well.

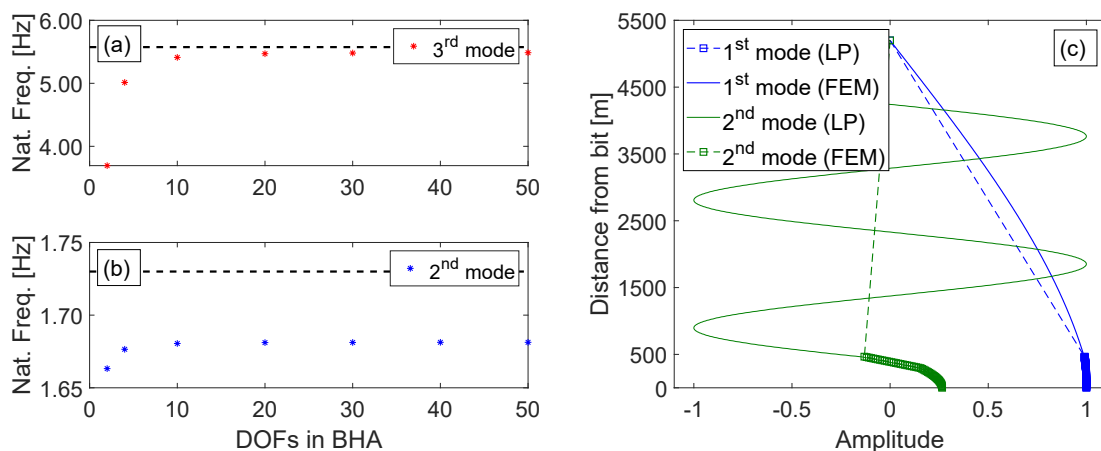


Figure 4: (a,b) Comparison between natural frequencies obtained with the lumped parameter model (LP) and the ones obtained by FEM (horizontal dashed lines). The DPs are discretized in 1 DOF and the BHA is flexible. (c) Mode shapes calculated for the first and second modes with the DPs discretized in 1 DOF and the BHA in 50 DOFs.

If more DOFs are used in both DP and BHA, the lumped parameter model can capture other natural frequencies with a good prediction quality. To show this, Fig. 5(a) shows the convergence of the 15th and 25th natural frequencies when both DPs and BHA are discretized. The number of DOFs in x-axis is the sum of the DOFs in DPs and BHA. The mode

shape of the 25th mode is shown in Fig. 5(b) when 120 DOFs are used in the DPs and 30 DOFs in the BHA. Good correspondence is obtained between the mode shape obtained with strategy B and the one from FEM.

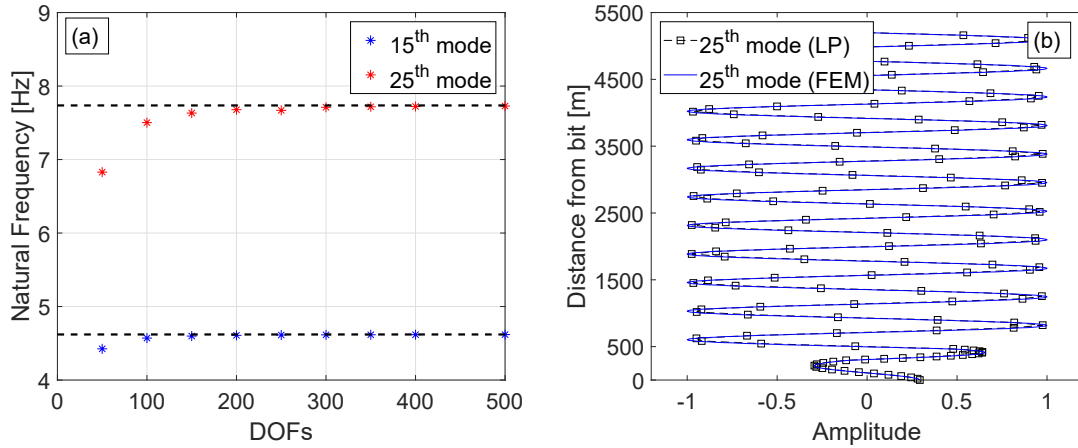


Figure 5: (a) Comparison between natural frequencies obtained with the lumped parameter model (LP) and the ones obtained by FEM (horizontal dashed lines). The DPs and BHA are considered flexible and discretized in multiple DOFs. (b) Mode shapes calculated for the 25th mode with the DPs discretized in 120 DOF and the BHA in 30 DOFs.

The severity of torsional vibration is often assessed by using the following coefficient:

$$S_{SS} = \frac{\max(\dot{\theta}_{bit}(t)) - \min(\dot{\theta}_{bit}(t))}{2\Omega}, \quad (12)$$

which measures the variation of bit rotational speed in the steady-state. In this work, the torsional vibration is considered severe when $S_{SS} > 80\%$. Using this coefficient, it is possible to construct a map which presents the torsional severity for each pair of applied W_{ob} and Ω . From this map, the critical value of $W_{ob,cr}$ can be defined for each rotational speed Ω applied at the top such that W_{ob} values higher than this produces severe vibrations. Figure 6(a) plots the critical value of $W_{ob,cr}$ for the dimensionful model. Different parameters of the drill-string are changed in order to evaluate the effect on the graph and it is noticed that curves change significantly. Figure ??(b) shows the same graph but for the dimensionless model, using the dimensionless quantities Π_1 and Π_2 . It is noticed that the use of these dimensionless quantities can reduce the sensitivity of torsional vibration severity analysis on drill-string parameters variations.

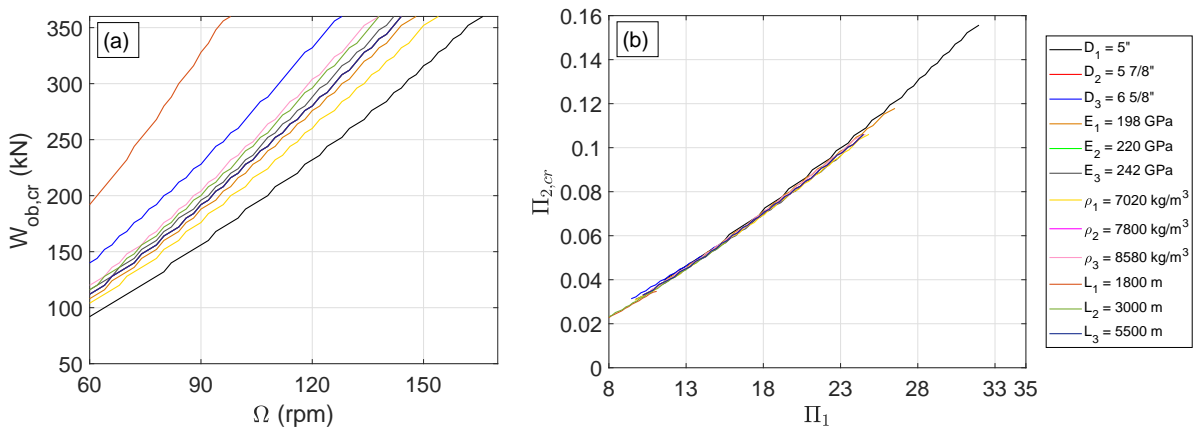


Figure 6: Torsional vibration severity map. (a) Dimensionful model, and; (b) Dimensionless model.

4. CONCLUSIONS

According to the results, lumped parameter models can efficiently describe the first mode with only one DOF if a proper strategy is used. Also, the increase of the DOFs in the drill-pipes is useful to describe more modes, but an increase only in BHA can mislead the conclusions. The use of more DOFs in both drill-pipes and BHA allows the calculation of more modes with good accuracy. In addition, the use of a dimensionless equation of motion could reduce the sensitivity

of torsional severity map to changes on drill-string parameters. Therefore, the use of dimensionless equations can lead to more general conclusions.

5. ACKNOWLEDGEMENTS

This study was financed in part by the Coordenação de Aperfeiçoamento de Pessoal de Nível Superior (CAPES) - Finance code 001 - Grant PROEX 803/2018, and the Brazilian agencies: Conselho Nacional de Desenvolvimento Científico e Tecnológico (CNPQ) - Grants 303302/2015-1, 400933/2016-0, Fundação Carlos Chagas Filho de Amparo à Pesquisa do Estado do Rio de Janeiro (FAPERJ) - Grant E-26/201.572/2014.

6. REFERENCES

- Germaý, C., Denoël, V. and Detournay, E., 2009. "Multiple mode analysis of the self-excited vibrations of rotary drilling systems". *Journal of Sound and Vibration*, Vol. 325, No. 1-2, pp. 362–381. ISSN 0022460X. doi: 10.1016/j.jsv.2009.03.017.
- Hong, L., Girsang, I.P. and Dhupia, J.S., 2016. "Identification and control of stick-slip vibrations using Kalman estimator in oil-well drill strings". *Journal of Petroleum Science and Engineering*, Vol. 140, pp. 119–127. ISSN 09204105. doi:10.1016/j.petrol.2016.01.017.
- J. P. Den Hartog, 1947. *Mechanical Vibrations*. McGraw-Hill, New York, third edit edition.
- Jansen, J.D. and van den Steen, L., 1995. "Active damping of self-excited torsional vibrations in oil well drillstrings". *Journal of Sound and Vibration*, Vol. 179, No. 4, pp. 647–668. ISSN 0022-460X. doi:10.1006/jsvi.1995.0042.
- Kamel, J.M. and Yigit, A.S., 2014. "Modeling and analysis of stick-slip and bit bounce in oil well drillstrings equipped with drag bits". *Journal of Sound and Vibration*, Vol. 333, No. 25, pp. 6885–6899. ISSN 10958568. doi: 10.1016/j.jsv.2014.08.001.
- Lobo, D.M., Ritto, T.G. and Castello, D.A., 2017. "Stochastic analysis of torsional drill-string vibrations considering the passage from a soft to a harder rock layer". *Journal of the Brazilian Society of Mechanical Sciences and Engineering*, Vol. 39, No. 6, pp. 2341–2349. ISSN 18063691. doi:10.1007/s40430-017-0800-2. URL <http://link.springer.com/10.1007/s40430-017-0800-2>.
- Nandakumar, K. and Wiercigroch, M., 2013. "Stability analysis of a state dependent delayed, coupled two DOF model of drill-stringvibration". *Journal of Sound and Vibration*, Vol. 332, No. 10, pp. 2575–2592. ISSN 0022460X. doi: 10.1016/j.jsv.2012.12.020.
- Navarro-López, E.M. and Cortés, D., 2007. "Sliding-mode control of a multi-DOF oilwell drillstring with stick-slip oscillations". *Proceedings of the American Control Conference*, pp. 3837–3842. ISSN 07431619. doi: 10.1109/ACC.2007.4282198.
- Navarro-lópez, E.M., Suárez, R., Navarro-Lopez, E.M. and Suarez, R., 2004. "Practical approach to modelling and controlling stick-slip oscillations in oilwell drillstrings". *Proceedings of the 2004 IEEE International Conference on Control Applications, 2004.*, Vol. 2, No. October 2004, pp. 1454–1460. ISSN 1085-1992. doi: 10.1109/CCA.2004.1387580.
- Richard, T., Germaý, C. and Detournay, E., 2007. "A simplified model to explore the root cause of stick-slip vibrations in drilling systems with drag bits". *Journal of Sound and Vibration*, Vol. 305, No. 3, pp. 432–456. ISSN 10958568. doi:10.1016/j.jsv.2007.04.015.
- Ritto, T.G., Aguiar, R.R. and Hbaieb, S., 2017. "Validation of a drill string dynamical model and torsional stability". *Meccanica*, Vol. 52, No. 11-12, pp. 1–9. ISSN 15729648. doi:10.1007/s11012-017-0628-y.
- Saldivar, B., Mondié, S., Niculescu, S.I., Mounier, H. and Boussaada, I., 2016. "A control oriented guided tour in oilwell drilling vibration modeling". *Annual Reviews in Control*, Vol. 42, pp. 100–113. ISSN 13675788. doi: 10.1016/j.arcontrol.2016.09.002.
- Tang, L., Zhu, X., Shi, C., Tang, J. and Xu, D., 2015. "Study of the influences of rotary table speed on stick-slip vibration of the drilling system". *Society of Petroleum Engineers*, Vol. 1, No. 4, pp. 382–387. ISSN 2405-6561. doi:10.1016/j.petlm.2015.10.004.
- Tucker, R.W. and Wang, C., 1997. "The Excitation and Control of Torsional Slip-Stick In the Presence of Axial-Vibrations". pp. 1–5. URL <http://www.lancs.ac.uk/users/SPC/Physics.htm>.
- Yigit, A. and Christoforou, A., 1998. "Coupled torsional and bending vibrations of drillstrings subject to impact with friction". *Journal of Sound and Vibration*, Vol. 215, No. 1, pp. 167–181. doi:10.1006/jsvi.1998.1617.

7. RESPONSIBILITY NOTICE

The following text, properly adapted to the number of authors, must be included in the last section of the paper:
The author(s) is (are) the only responsible for the printed material included in this paper.